Effect of lithium on optical and structure, characterization of nanostructured Fe_2O_3 thin films deposited by chemical spray pyrolysis technique

Z. S. Mahdi, Z. A. Abed*, R. M. Abdullah
Physics Department, College of Science, University of Diyala, Diyala, Iraq

Chemical spray pyrolysis (CSP) is employed to generate nanostructured undoped Fe2O3 and Fe2O3: Li films at varied doping levels. grain size rose as lithium concentration increased, increasing from 17.89 nm to 20.57 nm, while the dislocation density falls from 31.24 to 23.63, while the strain drops from 19.37 to 16.95 in the grown films acquired by XRD. The topography of the films was investigated using AFM. For the (Undoped Fe2O3, Fe2O3:1 % Li, Fe2O3:3 % Li), the Average Particle Size decreased to (78.2), (61.47), and (42.40) nm, respectively, whereas the Roughness Average decreased from 7.84 nm to 32.4 nm, Whilst the root root-mean-square (Rrms) values of the deposited films were (8.72, 8.00 and 4.19) nm. Optical characteristics such as transmittance and optical constants were determined using a UV-Visible spectrophotometer. The optical bandgap of Fe2O3 was reduced from 2.75 eV for Fe2O3 film to 2.60 eV for Fe2O3:3 % Li film. Lithium doping increases the absorption coefficient, whereas the Extinction coefficient and refractive index decreases with Lithium content.

(Received September 29, 2023; Accepted March 19, 2024)

Keywords: Fe_2O_3, Li, Thin films, CSP, Structural, Optical bandgap

1. Introduction

Hematite (Fe_2O_3) has a bandgap of roughly 2-2.2eV, allowing it to absorb about 40% of solar energy through its visible region. Fe_2O_3 is regarded a potential material for solar energy applications because of this aspect. Due to its abundance in nature, Fe_2O_3 is inexpensive and corrosion-resistant in both acidic and alkaline conditions [1]. Due to its dielectric qualities and breakthrough of having high thermopower simultaneously, this metal oxide has made its way into a variety of additional applications. [2-7]. By combining Fe^{2+} and Fe^{3+} and adding a base, iron oxides can be made. The size, shape, and content of iron oxide nanoparticles generated by chemical techniques are dependent on the type of salt utilized, such as chlorides [8-11]. The optical properties of Fe_2O_3 are significant for evaluating their optical and photo catalytic activity, which may suggest that the thin films are acceptable for usage in specific applications. [12]. Due to its high electron–hole recombination rate, - Fe_2O_3 has a low energy conversion efficiency. Many people suggested adding a small amount of a third ingredient to boost conversion efficiency [13-16]. The structural, optical, and morphological characteristics of Fe_2O_3 are all affected by deposition temperature [17]. Many researchers have worked on various Fe_2O_3 fabrication processes, including pulsed laser deposition [18], DC reactive magnetron sputtering [19], sol-gel [20, 21], and sputtering. [22], and thermal evaporation method [23], CVD [24], and CSP [25]. Chemical spray pyrolysis was employed in this study to produce undoped Fe_2O_3 films with varying lithium content. Based on structural, morphology, and optical properties, the films can be classified for various applications.

2. Experimental

CSP was used to prepare samples of lithium-doped Fe_2O_3 thin films. To prepare the coating solution, dissolve Fe chloride hexahydrate ($FeCl_2.6H_2O$) in 100 ml redistilled water to make a 1 M solution. Lithium had a volumetric (0, 1, 3) % ratio. The temperature of the substrate was 450 degrees Celsius. The layers were placed onto glass substrates that had previously been

* Corresponding author: zaidabdulhadi@uodiyala.edu.iq
https://doi.org/10.15251/DJNB.2024.191.443

chemically and ultrasonically cleaned. The deposition was improved by using the following parameters: spraying rate of 0.2 milliliters per spray, distance from adsorbent to hose of 30 centimeters, spraying time throughout each cycle of 10 seconds, the delay between successive sprays of 90 seconds, and carrier gas of filtered compressed air at a pressure of 105 Nm-2. According to gravimetric studies, the thickness was approximately 325 nm. X-ray diffractometer was used to examine the structural properties of the deposited thin films. AFM is gained to study film surface. then optical transmittance is recorded using double beam spectrophotometer.

3. Results and discussions

The X-ray pattern of Fe_2O_3 and Fe_2O_3: Li thin films is shown in Figure 1. Based on these findings, the polycrystalline structure can be seen in all thin films. All of the patterns have diffraction peaks around (232.22o, 35.71, 50.02, and 60.51), which correspond to the (220), (311), (421), and (521) preferred directions, respectively, which is consistent with JCPDS card number 39-1346. According to the peak intensity study, all the intended films had a preferred orientation along the (002) direction.

The grain size (D) can be estimated using Scherer's formula [26]:

$$D = \frac{K\lambda}{\beta\cos\theta} \tag{1}$$

where λ is the x-ray wavelength used, k = 0.9 and θ is Bragg angle and □□is FWHM (in radian). The grain size was 17.89 nm for the undoped and Lithium (3%) doped Fe_2O_3, while its value for Lithium (3%) doped Fe_2O_3 was 20.27 nm. Table (1) represents the structural parameters for all the deposited thin films.

The dislocation density (δ) in the film can be estimated using the following equation [27]:

$$\delta = \frac{1}{D^2} \tag{2}$$

Table 1. It was discovered that the density of dislocations () dropped from 31.24 to 23.63.

The film's strain (ε) can be calculated using the following equation [28]:

$$\varepsilon = \frac{\beta\cos\theta}{4} \tag{3}$$

Table 1. It showed that strain (ε) decreased from 19.37 to 16.95.

Structural parameters Sp were shown in Figure (2).

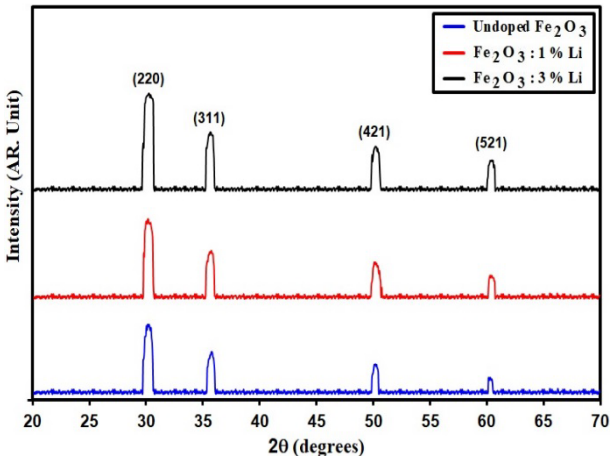

Fig. 1. XRD styles of grown films.

Table 1. D, optical bandgap and S_P of grown films.

Sample	2 θ (°)	(hkl) Plane	FWHM (°)	E_g(eV)	*D* (nm)	δ(× 10^{14}) (lines/m^2)	ε(× 10^{-4})
Undoped Fe_2O_3	30.22	220	0.46	2.75	17.89	31.24	19.37
Fe_2O_3: 1% Li	30.20	220	0.43	2.65	19.14	27.29	18.11
Fe_2O_3: 3% Li	30.00	220	0.40	2.60	20.57	23.63	16.95

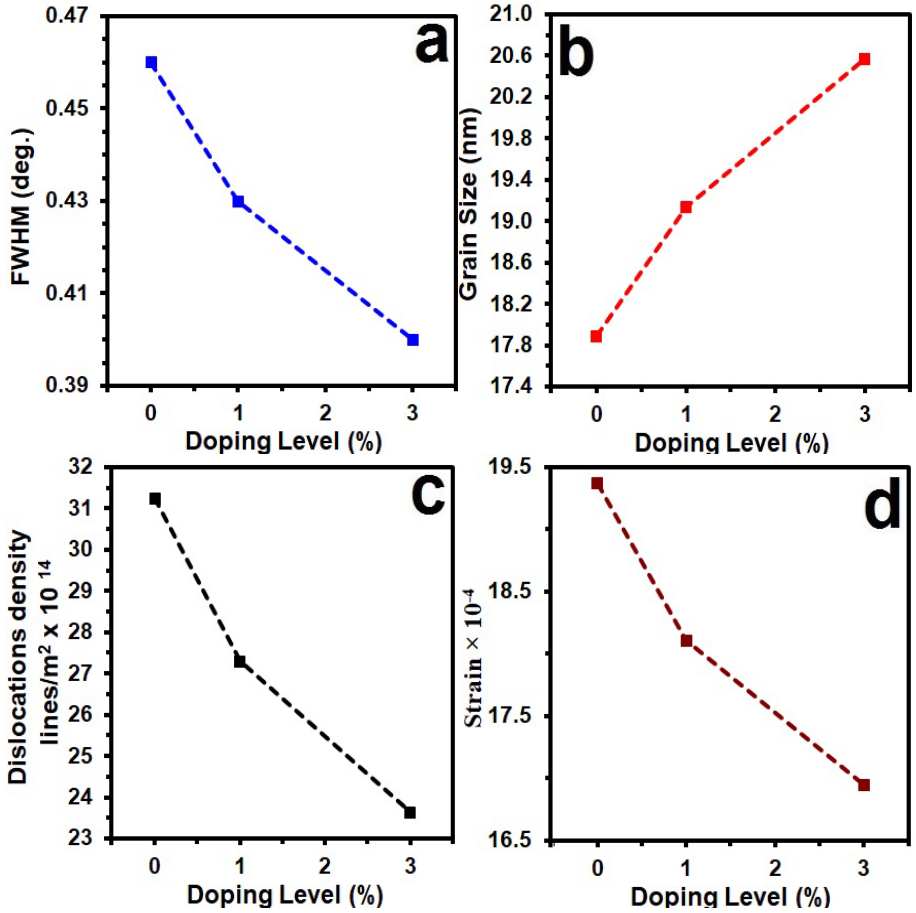

Fig. 2. S_P of the grown films.

AFM pictures of the intended films are offered in Figure 3. These photos show films dispersed equally in the form of microscopic granules with no gaps between them. A volumetric distribution of crystalline granules is shown in Figure 3 (a2, a2, and a3) [38, 39]. (c1, c2 and c3). For Undoped Fe_2O_3, Fe_2O_3: 1 % Li, and Fe_2O_3: 3 % Li, the average particle size P_{av} , average roughness (Ra), and root root-mean-square (Rrms) values are (78.20,61.47, and 42.40) nm, (7.84, 4.64, and 3.24) nm, and (8.72, 8.00, and 4.19) nm, respectively. The results show that Lithium content affects Ra and Rrms. The values of AFM parameters P_{AFM} are shown in Table 2.

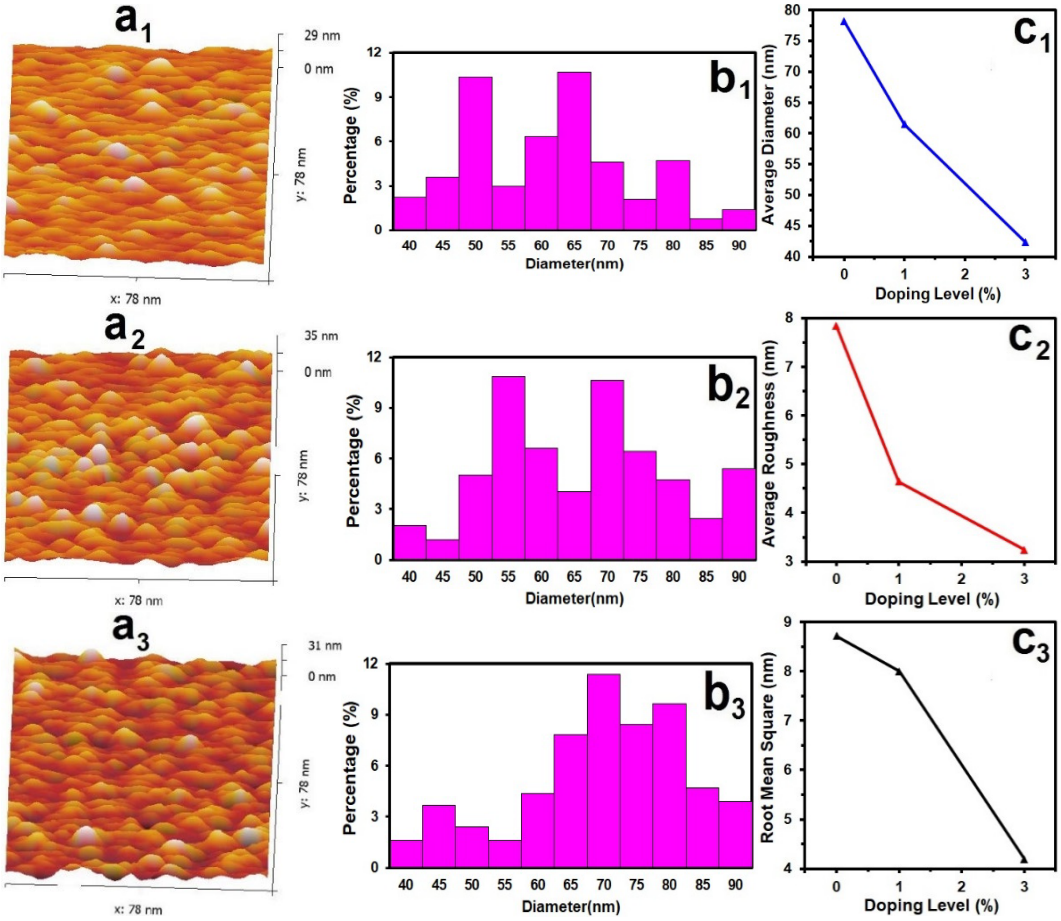

Fig. 3. AFM images and informations.

Table 2. P_{AFM} of the intended films.

Samples	P_{av} nm	Roughness Average (nm)	R_{rms} (nm)
Undoped Fe_2O_3	78.2	7.84	8.72
Fe_2O_3: 1% Li	61.47	4.64	8.00
Fe_2O_3: 3% Li	42.40	32.4	4.19

Undoped Fe_2O_3 and Fe_2O_3 optical transmission (T) spectra: The greatest transmission was around 80 % Undoped Fe_2O_3, while 3 % Lithium doped Fe_2O_3 decreases the transmittance (Fig. 4). This intriguing behavior could be related to the solubility of Lithium atoms in the Fe_2O_3 structure, and could indicate a rise in the localized impurity level in the Fe_2O_3 band gap as Lithium concentration is increased. [29].

The absorption coefficient (α) was specified by equation [30]:

$$\alpha = (2.303 \times A)/t \quad (4)$$

(t) is the film thickness. These films exhibit ($10^4 cm^{-1}$), which suggests direct transitions [31]. Figure 5 shows against photon energy (hν). The absorption coefficient rises as hν rises, and the absorption coefficient rises as Lithium doping rises.

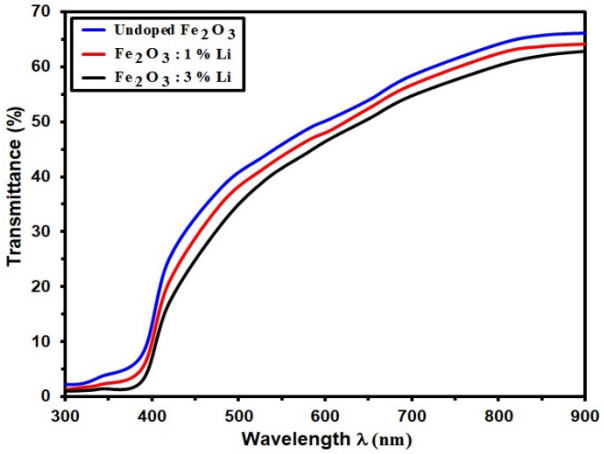

Fig. 4. Transmittance of the grown films.

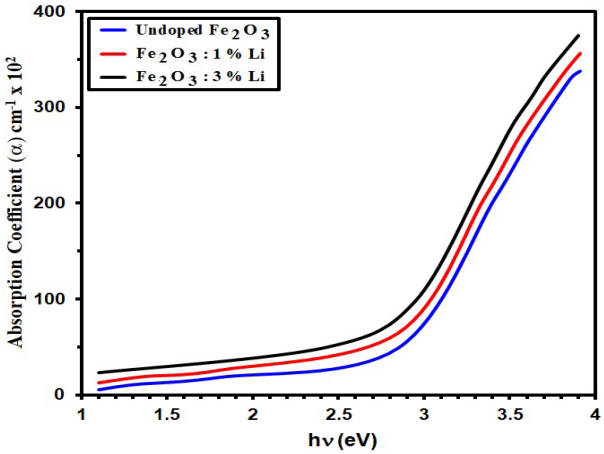

Fig. 5. α Vs hν of the prepared films.

Direct optical band gap is estimated using the Tauc 's equations [32]:

$$(\alpha h\upsilon) = A(h\upsilon - E_g)^{\frac{1}{2}} \tag{5}$$

where A is the constant, $(\alpha h\upsilon)^2$ against incident photon energy ($h\upsilon$), Fig. (6) show the plot of $(\alpha h\upsilon)^2$ versus $h\upsilon$ for the films under investigation. We can see that the calculated E_g for the undoped Fe_2O_3 was found to be around 2.75 eV.

The extinction coefficient (k) using the following relation [30]:

$$K = \frac{\alpha\lambda}{4\pi} \tag{6}$$

where λ is photon wavelength. Fig. (7) offered the variation of k with wavelength, which decreases with increased lithium doping.

The refractive index (n) can be gained from the reflectance (R) data using the relation [31]:

$$n = \frac{1+\sqrt{R}}{1-\sqrt{R}} \tag{7}$$

As shown in Fig. (8) n is influenced by increasing Lithium doping. by decreases as by increasing its value via Lithium doping.

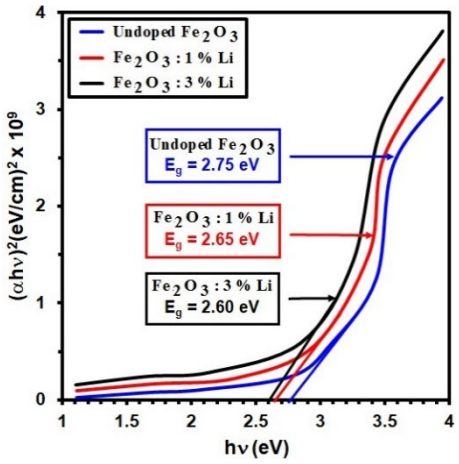

Fig. 6. $(\alpha hv)^2$ versus hv for the NiO with different Al doping.

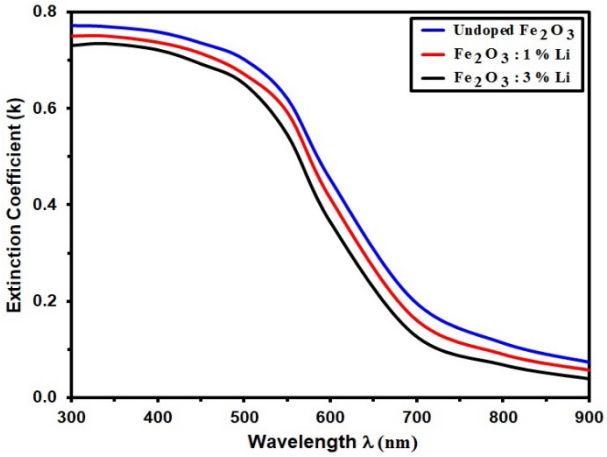

Fig. 7. (k) of the grown films.

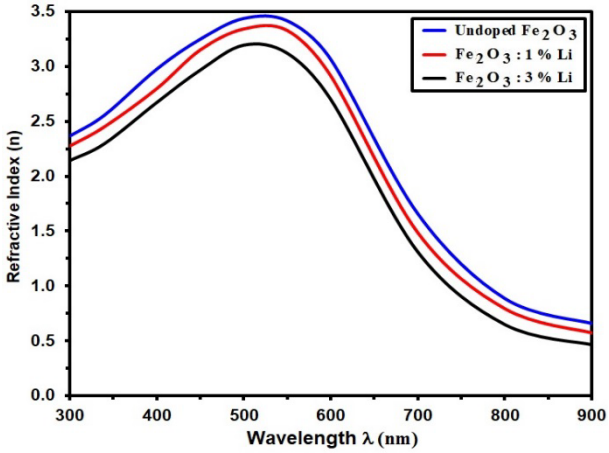

Fig. 8. n for grown films.

4. Conclusions

The structure of polycrystalline Nanostructured Fe_2O_3 and Fe_2O_3: Li films produced on a glass substrate by chemical spray pyrolysis is studied using XRD. All synthesized films have an XRD reflecting main peak at 2 = 30.22o, pointing in the direction of (220). grain size rose as lithium concentration increased, increasing from 17.89 nm to 20.57 nm, while strain decreased from 19.37 to 16.95 nm. Undoped Fe_2O_3 and Fe_2O_3: Li films nanostructures have a smooth surface morphology, and the Average Particle Size decreases as (78.2), (61.47), and (42.40) nm for the (Fe_2O_3, Fe_2O_3:1 % Li, Fe_2O_3:3 % Li), respectively. The transmittance decreases with Lithium doping, and the bandgap decreases with increases. Lithium doping increases the absorption coefficient, whereas the refractive index and extinction coefficient decrease.

References

[1] I.A. Raid, Y. Najim, M. Ouda, Spray Pyrolysis Deposition of α Fe_2O_3 Thin Film, e-J. Surf. Sci. Nanotech. 6 (2008) 96-98; https://doi.org/10.1380/ejssnt.2008.96

[2] L. F. Goncalves, L. S. R. Rocha, E. Longo, A. Z. Simões, J. Mater. Sci. Mater. Electron, 29 (2018) 784-793; https://doi.org/10.1007/s10854-017-7973-4

[3] R. Reveendran and M. A. Khadar, Mater. Chem. Phys., 219 (2018) 142-154; https://doi.org/10.1016/j.matchemphys.2018.08.016

[4] N. F. Habubi, K. A. Mishjil, H. G. Rashid, Atti. Dell. Fond Gior. Ron. 66, 6 (2011) 883-891.

[5] N. J. Mohmmed, N. F. Habubi, Int. lett. Chem. Phys. astron. 14, 1 (2014) 65-85; https://doi.org/10.56431/p-998luq

[6] J.A. Joseph, S.B. Nair, S.A. Mary, S.S. John, S. Shaji, R. R. Philip, Phys. Status Solidi, 259 (2021) 2100437; https://doi.org/10.1002/pssb.202100437

[7] A. L. Stroyuk, I. V. Sobran, S. Y. Kuchmiy, J. Photoch. Photobio. A. 192, 2-3 (2007) 98-104; https://doi.org/10.1016/j.jphotochem.2007.05.010

[8] N.V. Long, Y. Yang, M. Yuasa, C.M. Thi, Y. Cao, T. Nann, M. Nogami, RSC Adv 4 (2014) 8250-8255; https://doi.org/10.1039/c3ra46410e

[9] N.V. Long, Y. Yang, C.M. Thi, Y. Cao, M. Nogami, Colloids and Surfaces A: Physicochemical and Engineering Aspects 456 (2014) 184-194; https://doi.org/10.1016/j.colsurfa.2014.05.001

[10] R D Suryavanshi, S V Mohite, A A Bagade, K Y Rajpure, Materials Science and Engineering: B, 248 (2019) 114386; https://doi.org/10.1016/j.mseb.2019.114386

[11] V.V. Malyshev, A.V. Eryshkin, E.A. Koltypin, A.E. Varfolomeev, A.A. Vasiliev, Sensors and Actuators B: Chemical 19 (1994) 434-436; https://doi.org/10.1016/0925-4005(93)01031-X

[12] R. Cornell, U. Sh Wentmunn, The iron oxids: structure, properties, reation occurrence and uses, Darmstadt: wiley- VcH Gmb H and Co. KGaA, (2003).

[13] M. A. García-Lobato et al, Materials Science Forum. 644 (2010) 105-108; https://doi.org/10.4028/www.scientific.net/MSF.644.105

[15] C.D. Park, D. Magana, A. E. Stiegman, Chem. Mater. 19 (2007) 677-683; https://doi.org/10.1021/cm0617079

[16] Negar Khademi, M. M. Bagheri-Mohagheghi, Thermal Energy and Power Engineering. 2 (2013) 89-93.

[17] A.Z. Moshfegh, R. Azimirad, O. Akhavan, Thin Solid Films. 484 (2005) 124-131; https://doi.org/10.1016/j.tsf.2005.02.019

[18] S. D. Chavhan, S. V. Bagul, R. R. Ahire, N. G. Deshpande, A. A. Sagade, Y. G. Gudage, Ramphal Sharma, J. of Alloys and Compounds, 436 (2007) 400-406; https://doi.org/10.1016/j.jallcom.2006.09.126

[19] Langford JI, Wilson AJC (1978) J Appl Cryst 11:102-113; https://doi.org/10.1107/S0021889878012844

[20] S. Mathur, V. Sivakov, H. Shen, S. Barth, C. Cavelius, A. Nilsson, P.Kuhn, Thin Solid Films. 502 (2006) 88-93; https://doi.org/10.1016/j.tsf.2005.07.249

[21] E.L. Miller, D. Paluselli, B. Marsen, R.E. Rocheleau, Solar Energy Mater. And Solar Cells. 88 (2005) 131-144; https://doi.org/10.1016/j.solmat.2004.07.058

[22] Scherrer P (1918) Nachr Ges Wiss Go¨ttingen 26:98-100

[23] X.W. Li, A. Gupta, G. Xiao, G.Q. Gong, J. Appl. Phys. 83 (1998) 7049-7051; https://doi.org/10.1063/1.367547

[24] Sami Salman Chiad, Tahseen H. Mubarak, International Journal of Nanoelectronics and Materials, Volume 13, No. 2, 2020, PP. (221-232).

[25] Zaid A. Abed, Ali H. Al Dulaimi, Wafaa A. Shatti, Ahmed N. Jasim, Ziad T. Khodair, Sura Y. Khaleel, Journal of Ovonic Research, Vol. 17 (6), 2021, p. 581 – 587; https://doi.org/10.15251/JOR.2021.176.581

[26] Hassan, E.S., Mubarak, T.H., Chiad, S.S., Habubi, N.F., Khadayeir, A.A., Dawood, M.O., Al-Baidhany, I.A. Journal of Physics: Conference Series, 1294(2), 2019; https://doi.org/10.1088/1742-6596/1294/2/022008

[27] Dawood, M.O., Chiad, S.S., Ghazai, A.J., Habubi, N.F., Abdulmunem, O.M., AIP Conference Proceedings 2213, 2020; https://doi.org/10.1063/5.0000136

[28] Khadayeir, A. A., Hassan, E. S., Mubarak, T. H., Chiad, S.S., Habubi, N. F., Dawood, M.O., Al-Baidhany, I. A., Journal of Physics: Conference Series, 2019, 1294 (2) 022009; https://doi.org/10.1088/1742-6596/1294/2/022009

[29] Chiad, S.S., Habubi, N.F., Abass, W.H., Abdul-Allah, M.H., Journal of Optoelectronics and Advanced Materials **18**(9-10), 822 (2016).

[30] Ahmed, F.S., Ahmed, N.Y., Ali, R.S., Habubi, N.F., Abass, K.H. and Chiad, S.S. NeuroQuantology, 18 (3), 56-65, 2020; https://doi.org/10.14704/nq.2020.18.3.NQ20151

[31] Chiad, S.S., Noor, H.A., Abdulmunem, O.M., Habubi, N.F., Journal of Physics: Conference Series 1362(1), 2019; https://doi.org/10.1088/1742-6596/1362/1/012115

[32] M.R. Belkhedkar , A.U. Ubale, Y.S. Sakhare, Naushad Zubair and M. Musaddique, Journal of the Association of Arab Universities for Basic and Applied Sciences, 21, 38-44 (2016); https://doi.org/10.1016/j.jaubas.2015.03.001